

Jarðfræðafélag Íslands

HAUSTRÁÐSTEFNA 2002

haldin til heiðurs
Guðmundi E. Sigvaldasyni
sjötugum

Ágrip erinda og veggspjalda

Haldin á Nesjavöllum
18. október 2002

Jarðfræðafélag Íslands

HAUSTRÁÐSTEFNA 2002

haldin til heiðurs
Guðmundi E. Sigvaldasyni
sjötugum

Ágrip erinda og veggspjalda

Umsjón:
Sigurður Sveinn Jónsson
ssjo@os.is

Haldin á Nesjavöllum
18. október 2002

Efnisyfirlit

Accurate ¹⁴C datings of human bones influenced by mixed terrestrial/marine diet. A case story from Greenland	6
Árný E. Sveinbjörnsdóttir, J. Heinemeier, H.L. Nielsen, N. Rud, J. Arneborg and N. Lynnerup	
Hafsbotninn í Tjörnesbrotabeltinu.....	10
Bryndís Brandsdóttir, Robert Detrick, Guðrún Helgadóttir, Einar Kjartansson, Bjarni Richter, Karl Gunnarsson, Steinar Þór Guðlaugsson, Neal Driscoll og Graham Kent	
Inferring Volcano Dynamics and Magma Budget from Crustal Deformation Studies at Icelandic Volcanoes.....	11
Freysteinn Sigmundsson, Rikke Pedersen, Páll Einarsson, Erik Sturkell, Halldór Geirsson, Kurt L. Feigl, Þóra Árnadóttir, Carolina Pagli and Halldór Olafsson	
Jarðskjálftahrina á Tjörnesbrotabelti í september 2002.....	12
Gunnar B. Guðmundsson og Ragnar Stefánsson	
Kick'em Jenny: The Evolution of an Active Submarine Volcano	13
Haraldur Sigurdsson	
Fróðleg jarðsprunga og athugasemd um jarðskjálftann 1784.....	14
Kristján Sæmundsson	
Environmental Impact of the Silicic Part of the 871AD Vatnaöldur Eruption, Iceland	15
A. K. Mortensen, N. Óskarsson & G. Sverrisdóttir	
Advances in scientific drilling	16
Dennis L. Nielson	
Samband skjálftavirkni á Reykjaneshrygg við V-laga hryggi og jarðskorpumyndun.....	17
Páll Einarsson og Julia Rohlfs	
InSAR observations of crustal deformation in Iceland	18
Rikke Pedersen, Freysteinn Sigmundsson, Kurt Feigl, Carolina Pagli, Helene Vadon and Erik Sturkell	
Ion hydration and isotope fractionation in hydrothermal solutions	19
T. M.Seward	
The tephra layer from the 1362 Örefajökull eruption, SE-Iceland: A Plinian eruption associated with a caldera collapse.....	200
Rune S. Selbekk	

Basaltic Glass Dissolution.....	211
Sigurdur R. Gíslason, Eric H. Oelkers,; Domenik Wolff-Boenisch and Ólafur Arnalds ²¹	
Gler-innlyksur í kristöllum úr Búrfells-pikríti í Ölfusi	255
Sigurður Steinþórsson og Ingvar A. Sigurðsson	
Oxunarstig basaltbráðar sem fall af ildisþrýstingi, hitastigi og efnasamsetningu	266
Sigurður Steinþórsson og Örn Helgason	
Low-frequency earthquakes at the Torfajökull volcano, measured by a local network	277
Heidi Soosalu and Páll Einarsson	
Primary basalt mineral saturation in surface- and up to 90°C ground waters in Skagafjörður, N-Iceland.....	288
Stefán Arnórsson, Andri Stefánsson and Ingvi Gunnarsson	
Askja - still going down	322
Erik Sturkell, Carolina Pagli & Freysteinn Sigmundsson	

Accurate ^{14}C dating of human bones influenced by mixed terrestrial/marine diet. A case story from Greenland

Árný E. Sveinbjörnsdóttir¹, J. Heinemeier², H.L. Nielsen², N. Rud², J. Arneborg³ and N. Lynnerup⁴

¹Science Institute, University of Iceland, IS-107 Reykjavík, Iceland, ²Institute of Physics and Astronomy, University of Aarhus, DK-8000 Aarhus, Denmark, ³Department of Prehistory and the Middle Ages, The National Museum of Denmark, DK-1220, Copenhagen, Denmark, ⁴Laboratory of Biological Anthropology, The Panum Institute, University of Copenhagen, DK-2000, Copenhagen, Denmark

Introduction

The ^{14}C dating of bone is by now technically well established, relying on refined chemical extraction techniques combined with accelerator mass spectrometry (AMS) (e.g. Brown et al., 1988). Since very small samples of bone collagen can be dated with AMS, it has become possible to select the best samples from a skeleton, minimizing problems with degradation and contamination. If the bone collagen is of terrestrial origin, the measured (conventional) ^{14}C age is converted into a true calendar age by using the global tree-ring calibration curve (Stuiver and Polach, 1977). However, this simple procedure is not applicable when the bone collagen is derived in part from marine carbon which, due to the marine reservoir effect, appears several hundred ^{14}C years older than the corresponding terrestrial carbon. This seriously constrains the dating of bones of people who have had access to food protein from the sea. To extend the calibration of measured ^{14}C ages to marine bones one needs to know both the marine food fraction and the reservoir age, that is, the age difference between the atmosphere and the particular region of the sea at the time the protein was produced.

Previous investigations have shown that $\delta^{13}\text{C}$ of bone collagen can be used as an indicator of food composition. The $\delta^{13}\text{C}$ determined may be either the relative components of marine/terrestrial food protein or plants of C_3 and C_4 photosynthesis. The data compiled in Table 1 are for population groups from high northern latitudes where the $\delta^{13}\text{C}$ signal provides

Table 1: Bone collagen $\delta^{13}\text{C}$ values for population groups from northern regions

Locality	Period	type	N	$\delta^{13}\text{C}\text{‰}$ (VPDB)	Percent marine diet
Tuna, Sweden ^a	Viking age	Inland	7	-26.49±0.26	6
Leksand I, Sweden ^a	Medieval	Inland	11	-20.92±0.36	1
Leksand II, Sweden ^a	17th century	Inland	10	-20.69±0.33	4
Heidal, Norway ^a	Medieval	Inland	10	-20.6±0.3	5
Saskatchewan, Canada ^b	Prehistoric	Inland	50	-17.5±0.3	
British Columbia, Canada ^c	Prehistoric	Coastal	37	-13.3±0.4	91
West Greenland, Eskimos ^d	15th century	Coastal	8	-12.49±0.18	100

N is number of individuals in the population group, $\delta^{13}\text{C}$ is the relative deviation of the $^{13}\text{C}/^{12}\text{C}$ isotopic ratio from the VPDB standard. The variabilities in the $\delta^{13}\text{C}$ values are one standard deviation. Percent marine diet is calculated from $\delta^{13}\text{C}$ by linear interpolation between the $\delta^{13}\text{C}$ values -12.5‰ and -21‰, taken to be the endpoint values for purely marine and purely terrestrial (pure C_3) diet respectively.

^aThese data are for inland population from Sweden (Lidén and Nelson, 1994) and Norway (Johnsen et al., 1986) known to have negligible access to marine food.

^bThe less negative $\delta^{13}\text{C}$ average for this inland population is ascribed to admixtures of C_4 plants in diet (Lovell et al., 1986).

^cChrisholm et al., 1983

^dThis West Greenland Eskimo population were close neighbors to the Norse (Heinemeier and Rud, 1977). The $\delta^{13}\text{C}$ average is identical to our choice of endpoint value for 100‰ marine food.

a sharp distinction between marine and terrestrial food, since C_4 plants (with a different photosynthetic pathway and isotopic fractionation (Lowell et al., 1986) are not present in these areas. The $\delta^{13}C$ distribution for a single population group can be extremely narrow (standard deviation about 0,3‰, just a few times the measuring uncertainty). This means that the variability in metabolic isotope fractionation among individuals is negligible. Hence we conclude that differences in $\delta^{13}C$ of human bone collagen from high latitudes must reflect real differences in the average diet consumed by the individual over roughly 10 years, which represents the collagen turnover time in human bone.

The main aim of the project was to investigate the potential of using a simple linear interpolation between the endpoint (pure marine versus pure terrestrial) $\delta^{13}C$ values to 1) calculate the marine fraction of each individual, and 2) correct ^{14}C dates of mixed marine material. For this purpose, 27 human bones, 6 textiles and one ox bone were selected. All the samples were from the Settlements of the Norse people in Greenland and the human bones were selected from different parts of the Norse Settlements to cover the colonisation period from the late 10th to the middle 15th century.

^{14}C dates corrected for the reservoir effect

To establish a chronology within a short period high dating accuracy is needed. When dating human bones it is essential to be able to correct for the reservoir age, otherwise the bones of a Norseman who lived on salmon and seal will appear about 400 years older (when ^{14}C dated) than his twin brother, who lived on mutton and milk. If we were unable to account for the reservoir effect, a very “marine” Norseman from the end of the period might appear to be from the Landnam (initial settling) period. In our correction model we use a find in a churchyard at the locality identified as Herjólfssnes – the most southerly of the Norse settlements. During excavation in 1921 (Nörlund, 1924) three skeletons were found wrapped in woollen clothes, which had been used for the burials presumably because of shortage of wood for coffins. The textiles provide a unique opportunity to control the reservoir corrected ^{14}C age of the bones. The ^{14}C dates on a single thread of wool from each dress show that the graves are contemporaneous as expected from their relative positions.

Since sheep’s wool is of terrestrial origin, there is no reservoir correction and the graves are reliably dated to AD 1430±15 years – which makes it the youngest date so far with solid evidence of Norse presence in Greenland. One of the skeletons, a young woman (20-25 years), had an uncorrected ^{14}C age which was 420 years older than her clothes and would place her shortly after Landnam. The two other skeletons, a child and an older woman, were approximately 250 years older than their clothes. However, the $\delta^{13}C$ values of the bones indicate a marine content of 78% for the young woman and about 55% for the two others. By subtracting the corresponding fraction of a fully marine reservoir age of 450 years from the bone ^{14}C date of each of the three individuals we obtain reservoir corrected dates, which then become identical with those of their clothes in all three cases (Fig.1). Fuller description of the correction model and archaeological interpretation is given in Arneborg et al. (1999).

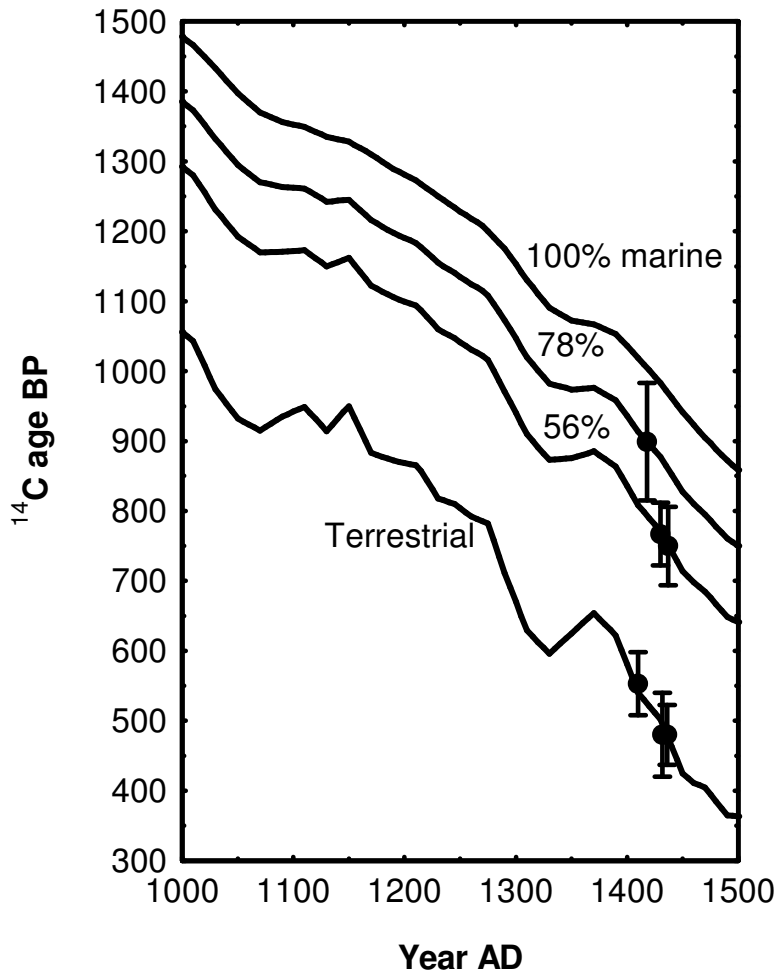


Figure 1. ¹⁴C calibration curves. Terrestrial curve is based on tree-ring measurements (Stuiver and Braziunas, 1993). Marine curve (100%) is a model calculation for the mixed layer of the ocean (Stuiver and Braziunas, 1993). Curves labelled 78% and 56% marine are interpolations. The data points are measured ¹⁴C ages of the 3 bone/cloth pairs from the Norse churchyard of Herjolfsnes, Greenland. The cloth data are plotted on the terrestrial curve. The $\delta^{13}\text{C}$ of the bone samples showed marine fraction of 55%, 56% and 78%. By assuming each bone/cloth pair to be of identical calendar age, the mixed-layer curve was adjusted by an upwards parallel shift to make the interpolated curves fit the bone data points. The displacement is $\Delta R=50$ yr, corresponding to a reservoir age varying between 400 and 500 ¹⁴C yr for the time range shown.

Stable carbon isotopes: a key to diet

High precision measurements on the stable carbon isotopes were performed on the mass-spectrometer at the Science Institute, University of Iceland. The results shown on Figure 2 show that the Greenland Norse data nearly cover the entire range between the terrestrial people from Norway and Sweden and the marine Eskimos from the Southwest coast of Greenland. Translated into diet composition, the corresponding range of marine food is as large as 20-80%. This variation in diet is exceptionally high for a single culture in a very limited period of time. It could be due to individual preferences, possibly in connection with social differences, or it might reflect a temporal trend caused for example by a steady deterioration of the regional climate during the period as evidenced by recent ice-core research (D-Dahl-Jensen et al, 1998).

When all the ¹⁴C dates of the human bones have been corrected for the reservoir effect after our correction model (Fig.1) a firm chronology appear. The large differences in the marine content of the Norseman bones (Fig. 2) represents a striking increase in the Norse population's dependence on sea food during the period from Landnam till the depopulation of the settlements 4-500 years later. In the beginning, the diet of the settlers is approximately 20% marine – more or less like that of contemporaneous Norwegians. Towards the end of the period, an adaptation to marine resources has taken place – up to 80% of the level observed for contemporaneous Eskimos.

Human bone collagen

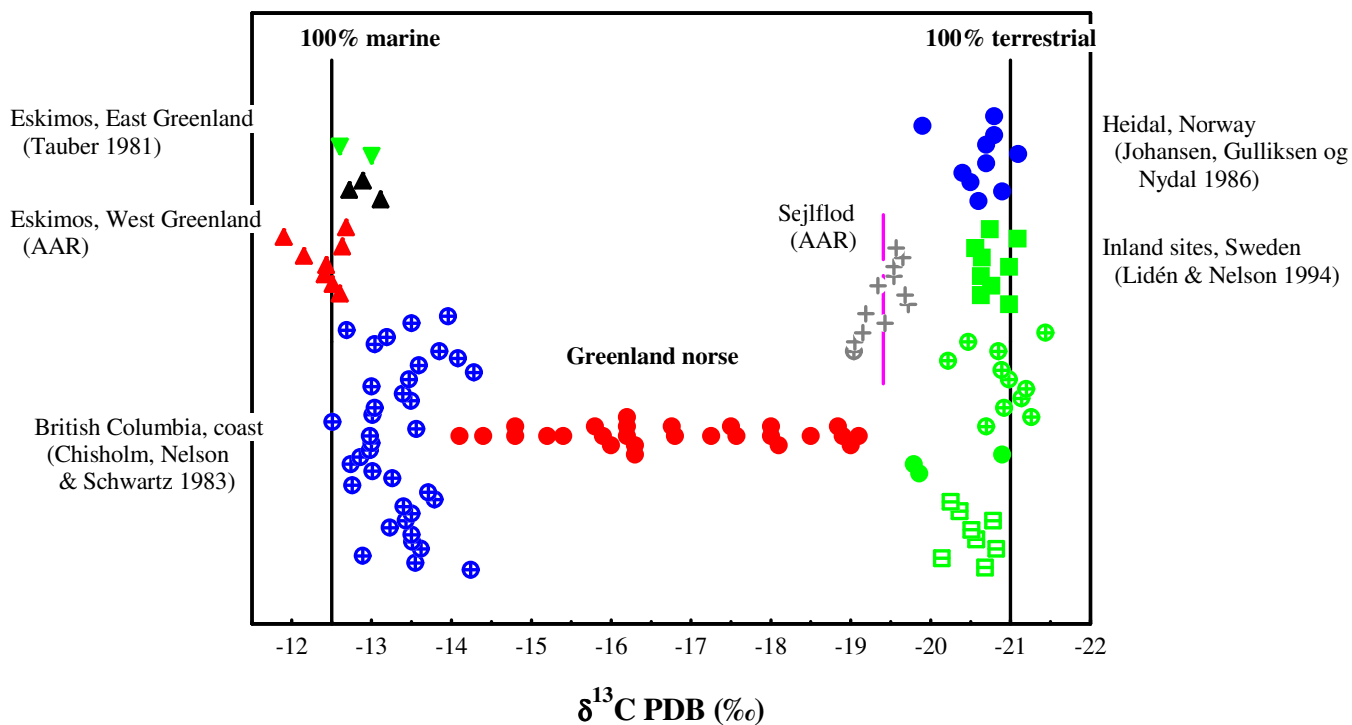


Figure 2. The plot shows how $\delta^{13}\text{C}$ (x-axis) clearly distinguishes people who have eaten terrestrial food from those who have eaten marine food (the y-axis only indicates grouping of the individual data series). The Greenland Norse data cover nearly the full range between the marine and terrestrial extremes.

References

- Arneborg et al. Radiocarbon 41 (1999) 157
- Brown et al. Radiocarbon 30 (1988) 171
- Chisholm et al. Current Anthropology 24 (1983) 396
- D-Dahl-Jensen et al. Science 282 (1998) 268
- Heinemeier and Rud Grønland 5-7 (1997) 232
- Johansen et al. Radiocarbon 28 (1986) 754
- Lidén and Nelson Fornvannen 89 (1994) 14
- Lovell et al. Archaeometry 28 (1986) 51
- Nörlund, Meddelelser om Grønland 67 (1924) 1
- Stuiver and Braziunas Radiocarbon 35 (1993) 137
- Stuiver and Polach Radiocarbon 19 (1977) 3

Hafsbotninn í Tjörnesbrotabeltinu

Bryndís Brandsdóttir(1), Robert Detrick(2), Guðrún Helgadóttir(3), Einar Kjartansson(3), Bjarni Richter(4), Karl Gunnarsson(4), Steinar Þór Guðlaugsson(4), Neal Driscoll(5) og Graham Kent(5)

(1)Raunvísindastofnun Háskólans, Haga, Hofsvallagötu 53, 107 Reykjavík, (2)Woods Hole Oceanographic Institution, Woods Hole, USA, (3)Hafrannsóknastofnun, Skúlagötu 4, 101 Reykjavík, (4)Orkustofnun, Grensásvegi 9, 108 Reykjavík, (5)Scripps Institution of Oceanography, Californíuháskóla., San Diego, USA

Tilkoma hafrannsóknaskipsins Árna Friðrikssonar, sem búið er fjölgeislamæli (Multibeam Echo Sounder) hefur opnað nýja möguleika í hafsbotnsrannsóknum. Með samþættingu endurkastsmælinga og nákvæmra korta af yfirborði hafsbotnsins má fá þrívíddarmyndir af misgengjum og setlögum sem varpað geta nýju ljósi á brotahreyfingar á nútíma (Hólósen) og jafnvel lengra aftur í tímann. Nýlegar fjölgeisla- og endurkastsmælingar á landgrunni Norðurlands hafa þannig veitt nýja innsýn á flókið brotabelti, kennt við Tjörnes, sem tengir nyrðra gosbeltið við Kolbeinseyjarhrygg.

Tjörnesbrotabeltið nær frá Skagagrunni í vestri, austur á Melrakkaslétu og frá Eyjafirði í suðri, norður undir Kolbeinsey. Þrjú sigdalir, Eyjafjarðaráll, Skjálfandadjúp-Skjálfandaflói og Öxarfjörður skera landgrunn brotabeltisins. Sigdalirnir, sem allir hafa norðlæga stefnu, afmarkast að sunnanverðu af Dalvíkur og Húsavíkur-Flateyjar sniðgengjunum og að norðanverðu af Grímseyjarbeltinu, þar sem saman fléttast eldvirkni, siggengi og sniðgengishreyfingar. Stærstu siggengin er að finna í hlíðum Eyjafjarðaráls. Þau greinast í NNA-SSV og NV-SA syðst í álnum þar sem Húsavíkur-Flateyjar sniðgengið gengur inn í hann. Brotabeltin í Eyjafjarðaráll, Skjálfanda, og Öxarfirði endurspeglar gliðunarvirkni í þeim öllum á nútíma. Ríkjanandi skjálftavirkni síðustu áratuga er þó aðallega bundin við misgengin í syðri sigdal Eyjafjarðaráls og Grímseyjarbeltið. Húsavíkur-Flateyjar sniðgengið greinist í þrjú meginhluta. Lóðrétt færsla á sniðgenginu minnkar til austurs frá Eyjafjarðaráll og er einnig viðsnúin (til suðurs) í Skjálfanda. Erfitt er að greina misgengið á yfirborði austast í Skjálfandaflóa þar sem lóðrétt færsla á því er lítil sem engin. Það sést þó greinilega í setlögnum. Síðustu landskjálftar á þessu svæði urðu árið 1872. Skjálftavirkni liggur aðallega eftir vesturjaðar Skjálfanda, norður að Grímsey (Álkantur austari).

Endurkastsmælingar sýna að setlagabykkt er mun meiri í álum og fjörðum. Landgrunnið sjálft er að uppistöðu hraunlagastafla og harðnað jökulberg en setið situr í álnum. Setlagabykkt er mun meiri í Skjálfandaflóa en í Eyjafjarðaráll. Set frá nútíma einkennist af 10-25 m þykku, ljósleitu lagi sem liggur ofan á 5-10 m þykku, mun dekkra lagi sem við teljum myndað út jökulhlaupaseti frá lokum síðustu ísaldar. Þar undir er sterkur endurkastsflötur, sennilegast jökulberg. Nokkuð er um endurkastsfleti innan efsta og ljósasta hluta lagsins sem falla saman við helstu öskulög í borkjörnum, þ.e. H1, H3, Saksunarvatn og Vedde gjóskuna. Yngsta setsyrpan er þykkust í Öxarfirði sem endurspeglar mun meiri framburð þangað en til Skjálfandaflóa og Eyjafjarðaráls. Þessa aukningu má rekja til Jökulsár á Fjöllum og jökulhlaupa niður farveg hennar, bæði af völdum jökulstíflaðra vatna og frá eldsumbrotum undir Vatnajökli.

Landslagi Kolbeinseyjarhryggjar og Grímseyjarbeltisins svipar mjög til nyrðra gosbeltisins og Reykjanesskaga. Upphleðslumiðjur (megineldstöðvar) með sprungusveimum (sigdölum) og gígaröðum liggja skástígt eftir plötuskilunum. Greina má þrjú kerfi frá Grímsey að hryggnum. Upphleðsla hefur verið mest á þrískilum Eyjafjarðaráls, Kolbeinseyjarhryggjar og Grímseyjarbeltisins.

Ofangreint verkefni samtvinnar grunnrannsóknir og þróunarstarf á sviði hafsbotnsrannsókna, þar sem við höfum verið eftirbátar annarra þjóða. Mælingarnar efla skilning okkar á gerð hafsbotnsins, eðli brotahreyfinga, virkni jarðhitasvæða, setmyndun á landgrunninu og tilvist hugsanlegra gasuppstreymissvæða.

Inferring Volcano Dynamics and Magma Budget from Crustal Deformation Studies at Icelandic Volcanoes

Freysteinn Sigmundsson¹, Rikke Pedersen¹, Páll Einarsson², Erik Sturkell³, Halldór Geirsson³, Kurt L. Feigl⁴, Þóra Árnadóttir¹, Carolina Pagli¹⁺² and Halldór Olafsson¹

(1) Nordic Volcanological Institute, (2) Science Institute, University of Iceland, (3) Icelandic Meteorological Office, (4) Centre National de Recherche Scientifique, Toulouse, France.

Crustal deformation studies of Icelandic volcanoes conducted for over 30 years provide an extensive data set, complementary to seismic observations. The geodetic studies are continuously expanding and cover now most of the active volcanic areas. Current measurements include campaign and continuous GPS, extensive InSAR studies, optical leveling tilt, and borehole strain. The measurements have revealed different styles of deformation at more than 15 volcanoes. They help quantify the location and volume of magma intrusions, as well as deflation and dike volumes associated with eruptions. The conventional elastic spherical-source Mogi model has successfully been used to fit many inflation/deflation episodes. The estimated volumes of transported magma is typically a small fraction of a cubic kilometer. Despite precise measurements of surface deformation fields, uncertainties on the estimated volumes are large because of possible inelastic effects and potentially complicated source geometry. The measurements have shown that the plumbing systems of the volcanoes are widely different, being influenced by the tectonic setting and time since last major magma recharging of the systems. Many of the volcanoes are presently not deforming, but some do have persistent local deformation sources due to shallow magma chambers whereas others deform episodically. Some of the continuously active sources are deflationary and are at least partly related to cooling of a magma chamber. For example, Askja volcano has been deflating at least since 1983 at a rate of about 5 cm/year. In many cases magma movements have triggered seismic activity, but in greatly varying amounts depending on several factors such as depth of the deformation source and the regional stress field. One of the smallest observed intrusion volumes, that of the Hengill volcanic area in 1994-1998, was associated with the highest seismic activity, because of high regional stress.

Jarðskjálftahrina á Tjörnesbrotabelti í september 2002

Gunnar B. Guðmundsson og Ragnar Stefánsson

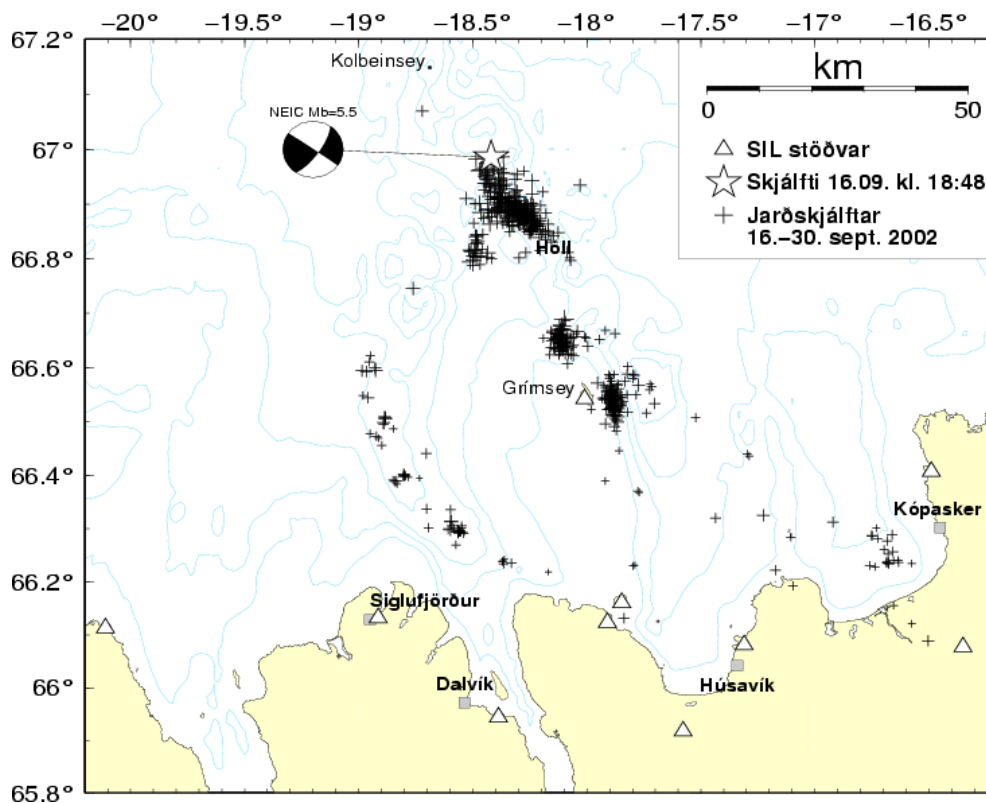
Veðurstofu Íslands, Bústaðavegi 9, 150-Reykjavík

Tjörnesbrotabeltið er brotabelti sem tengir saman norður gosbeltið og Kolbeinseyjar-hrygginn. Þann 16. september 2002 kl. 18:48 varð jarðskjálfti sem mældist 5.5 að stærð og fannst víða um Norðurland. Upptök skjálftans voru milli Grímseyjar og Kolbeinseyjar, um 53 km NNV af Grímsey (sjá mynd hér neðar). Skjálftinn fannst allt frá Sauðárkróki í vestri til Þistilfjarðar í austri og langt inn í innsveitir Eyjafjarðar. Bandaríska jarðfræðistofnunin (NEIC) mat stærð skjálftans $M_b=5.5$ og einnig brot-lausn þar sem annar mögulegur brotflöturinn hefur stefnuna $N35^\circ A$ og hallar 73° til SA og hinn u.þ.b. lóðréttur brotflötur með stefnu $N125^\circ A$. Í framhaldi af skjálftanum urðu margir eftirskjálftar. Stærsti eftirskjálftinn varð þann 17. september kl. 12:40 og hafði stærðina $M_b=4.4$. Upptök eftirskjálftanna dreifðust á um 15 km langt NNV-SSA skjálftabelti sem nær norður frá upptökum stóra skjálftans og suður að Hólnum. Samhliða og í framhaldi af þessari hrinu urðu skjálftahrinu um 15 km NNV af Grímsey og um 5 km austur af Grímsey. Einnig voru skjálftar um 20 km suður af upptökum stóra skjálftans og í Eyjafjarðarál. Engin gosórói sást á mælum í þessari skjálftahrinu.

Þetta er stærsta skjálftahrina norðan Grímseyjar síðan SIL jarðskjálftamælistöðvar voru settar upp á Norðurlandi í desember 1993. Vitað er um jarðskjálta að stærð 6,3 sem varð 23. ágúst 1921 kl. 20:17 og átti upptök um 50 km norður af Grímsey (Kjartan Ottósson, 1980), líklega á svipuðum slóðum og þessi jarðskjálfti.

Heimild:

Kjartan Ottósson, 1980. Jarðskjálftar á Íslandi 1900-1929. Raunvísindastofnun Háskólans, RH-90-05.



Kick'em Jenny: The Evolution of an Active Submarine Volcano

Haraldur Sigurdsson

Graduate School of Oceanography, University of Rhode Island, Narragansett, RI 02882, USA.

Submarine arc volcanoes constitute an important component of active island arc systems. Their activity contributes to the formation of thick volcanoclastic sequences, provides sites for hydrothermal mineralization, and may be responsible for the introduction of biogeochemically significant components such as Fe into the upper water column. In shallow water the activity of submarine arc volcanoes pose significant volcanic hazard. Kick'em Jenny is a submarine volcano in the Lesser Antilles arc. It has erupted at least 12 times since 1939 and is the most active volcano in the West Indies. The most recent eruption took place in December, 2001. Submersible dives on the crater revealed a spectacular bacterial bloom after the 1988 eruption. With a summit depth of only 180 meters, Kick'em Jenny provides a unique natural laboratory to study the activity and emergence of a young volcanic island. The volcano lies in a critical depth zone where eruptions can become more explosive in nature as it nears the surface. Dredge and "grab" samples from Kick'em Jenny reveal that it has produced a range of magma types, from olivine basalts to andesites, but its volcanics are highly unusual in some respects. The great abundance of amphibole megacrysts in the basalts have variously been attributed to high volatile content or the assimilation of xenocrysts from crustal rocks. Similarly the highly radiogenic isotope character has been interpreted to reflect the role of subduction-derived fluids and crustal contribution from crust-derived subducted sediments.

Multi-beam surveying in March 2002 has revealed evidence of a potentially widespread hazard from large-scale flank failure and submarine debris avalanche. The discovery of a major 4.5 km wide horse-shoe shaped crater or arcuate scarp surrounding Kick'em Jenny indicates that a large sector collapse has occurred. There is a good correlation between the width of an arcuate crater and the volume of its associated deposit over a range of crater sizes from less than 1 km to 10 km. Based on this relationship the volume of a deposit associated with the 4.5 km wide arcuate structure at Kick'em Jenny should be 10 km^3 . For known debris avalanches there is also a good correlation between deposit volume and total runout. A 10 km^3 debris avalanche would be expected to travel at least 50 km from source. Consequently, we would expect to find a large debris avalanche deposit in the deep part of the Grenada Basin to the west. The large inferred volume of the Kick'em Jenny debris avalanche raises questions about the nature of the structure that may have collapsed. Was the collapse confined to the submarine flanks or was there a pre-existing suberial edifice -- an island? Using the inferred volume of 10 km^3 it is possible to estimate the height of a collapse cone with a given diameter based on simple geometric relations. For example, a 10 km^3 cone with a basal diameter of 4.5 km would have an elevation of approximately 2 km. If the present cone of Kick'em Jenny was replaced by such a structure it would likely form a subaerial edifice a few hundred meters above sealevel.

Fróðleg jarðsprunga og athugasemd um jarðskjálftann 1784

Kristján Sæmundsson, Orkustofnun

Í Hveragerði var jarðsprunga merkt á skipulagsuppdrátt eftir skjálfta sem þar ollu tjóni vorið 1947. Stærstu skjálftarnir voru rúmlega 4 að stærð (Eysteinn Tryggvason 1978), og upptökin hafa sennilega verið á sprungunni sem liggur frá hverasvæðinu norður í Svaða. Sprungan sem merkt var á uppdráttinn er 200 m vestar og var dregin sem bein lína gegnum hveru neðan við Hamarinn og í réttinni suðvestan við þorpið. Pálmi Hannesson, Steinþór Sigurðsson og Sigurður Þórarinnsson voru á sínum tíma fengnir til að meta afleiðingar skjálftanna fyrir framtíðarskipulag og vöruðu þá við þessari sprungu. Skyldi sérstök aðgát höfð ef byggt yrði á eða nærri henni. Í haust kom loks að því að jarðskjálftasprunga þessi yrði sýnileg. Nærri suðurenda hennar þar sem réttin eitt sinn var er verið að undirbúa húsbyggingar þar sem nú heitir Réttarheiði. Í suðvestasta grunninum kom í ljós opin sprunga í hraunklökk. Hraunið sem þarna er á yfirborði er Hellisheiðarhraun B/C, en það er rúmlega 5.000 ára gamalt (Jón Jónsson 1977). Þegar dýpra var grafið kom í ljós að hraunið er 1 m á þykkt og undir því mold og síðan Hellisheiðarhraun A sem er um 10.000 ára (Jón Jónsson 1989). Sprungan var 10 cm víð í B/C-hrauninu, en 28 cm í A-hrauninu og stefndi N5-7°A. Missig var ekki á henni, en færslan var í stefnu N110°A. Þess má geta til að á nútíma hafi amk. þrívægis orðið hnik á þessari sprungu og þá um 10 cm í hvert sinn. Af öskulögum ofan á B/C-hrauninu má ráða hvenær hreyfing hafi orðið á henni eftir að það rann.

Í riti Þorvaldar Thoroddsen um jarðskjálfta á Suðurlandi (1899) segir um jarðskjálftann 1784: “Óvanaleg ólga kom í hveru nálægt Skálholti, en hjá Reykjavöllum í Biskupstungum hurfu hverar, sem áður voru”. Heimildir hans voru Magnús Stephensen (1785) varðandi hverina hjá Skálholti og Hannes Finnsson (1896) um þá hjá Reykjavöllum. Fáum sem nú lesa blandast hugur um hver skýringin muni vera á því sem þarna er lýst, því þetta sáum við gerast í skjálftunum 2000: Þurrð varð í hverum norðaustan og suðvestan við skjálftaupptök og – sprungu, en rennsli jókst í norðvestur- og suðausturgeirunum. Því má ætla að upptakasprunga skjálftans 14. ágúst sem þessu olli hafi legið norður-suður á milli hveranna í Skálholti og á Reykjavöllum og þá suður yfir Vörðufell, en vestan í því segir Hannes Finnsson að fallið hafi 36 skriður. Ef litið er á tjónasvæðið sem Sveinbjörn Björnsson (1978) teiknaði eftir heimildunum kemur í ljós að sprunga á þessum stað kemur illa heim við tjónasvæðið. Til þess er hún of vestarlega. Hins er svo að geta að sprungur miklar komu í jörð í Efri-Holtum, miklu austar og myndu falla betur að tjónasvæðinu. Því má álykta að þarna hafi orðið tveir skjálftar með örskömmu millibili og hafi allt að 10 km verið á milli upptakanna. Þegar tjónakortið er skoðað má sjá fleiri líkleg dæmi um þetta sama.

Eysteinn Tryggvason 1978. Jarðskjálftar á Íslandi 1940-1949. Raunvísindastofnun Háskólans RH-78-22, fjölrít 51 bls.

Hannes Finnsson 1796. Mannfækkun af hallærum á Íslandi. – Rit þess Kgl. Ísl. Lærdóms-lista Félags 14, 30-226.

Jón Jónsson 1977. Reykjafellsgígir og Skarðsmýrarhraun á Hellisheiði. – Náttúrufræðingurinn 47, 17-26.

Jón Jónsson 1989. Hveragerði og nágrenni, jarðfræðilegt yfirlit. – Rannsóknastofnunin Neðri-Ás, skýrsla 50, 56 bls.

Magnús Stephensen 1785. Kort Beskrivelse over den nye Vulkans Ildsprudning . . i Aaret 1783, 148 bls.

Pálmi Hannesson og Steinþór Sigurðsson 1948. Er ráðlegt að halda áfram að byggja í Hveragerði ? Syra 2, 1, 22-23, (nefndarálit).

Sveinbjörn Björnsson 1978. Í “Landskjálfti á Suðurlandi”, skýrsla vinnuhóps. Almannavarnir ríkisins AV-1, 07-78, 54 bls.

Þorvaldur Thoroddsen 1899. Jarðskjálftar á Suðurlandi, 199 bls.

Environmental Impact of the Silicic Part of the 871AD Vatnaöldur Eruption, Iceland

A. K. Mortensen, N. Óskarsson & G. Sverrisdóttir

Nordic Volcanological Institute, Grensásvegur 50, 108 Reykjavík, Iceland

The atmospheric injection of volcanic ash and gas from explosive volcanic eruptions can have an impact on the global climate. On a regional scale such events can have an impact on people and livestock, which are directly exposed to the fallout phase.

The silicic part of the Settlement Layer forms a widespread, thin layer, which covers $>11.500\text{km}^2$ of the southwestern part of Iceland. The silicic part of the Settlement Layer represents the early, plinian stage of the 871AD Vatnaöldur eruption, which was extruded from within Torfajökull, Southern Iceland. The silicic phase of the 871AD Vatnaöldur eruption was triggered by the lateral injection of basaltic magma from the 42km long, discontinuous Vatnaöldur fissure into the magma chamber of the Torfajökull central volcano. The Vatnaöldur fissure is part of the Veidivötn fissure swarm, and these simultaneous Veidivötn-Torfajökull eruptive events have occurred with a 500-800 year interval; the last three eruptions dated 150AD, 871AD and 1477AD (Larsen, 1984).

During transport of volcanic gas and tephra through the volcanic plume, parts of the volcanic gasses are adsorbed onto the surface of ash particles. Deposition of tephra contaminated with toxic volatiles, particularly fluorine, poses a hazard in the area of tephra fallout.

To evaluate the environmental impact of the silicic part of the 871AD Vatnaöldur eruption we estimate the volume of erupted tephra and volcanic gasses (SO_2 , HCl and HF) from the deposit characteristics and by the petrologic method, respectively. We combine these volume estimates with the surface area of the particle population of the deposit in an attempt to assess the environmental impact this eruption had in the fallout zone.

Advances in scientific drilling

Dennis L. Nielson, DOSECC

Scientific investigations have long used drilling as a tool for making subsurface observations and collection of samples of fluid and rock. Many of these efforts have resulted in important concepts that are today widely applied in commercial applications including geothermal development. Current topics of research involving drilling include determination of paleoclimate history using samples from modern lakes, measurement of stress and strain rates along major faults, sophisticated monitoring of faults and volcanoes and evaluation of volcanic and associated geothermal processes. The Iceland Deep Drilling Project falls in this category.

Overall, scientific drilling is expanding from an activity focused on the collection of samples from the earth's crust to include long-term observation of earth processes. There are two aspects that have influenced this change. First, drilling is expensive, and it is necessary to maximize the scientific value of holes drilled. In the private sector, wells represent capital investments that are expected to produce returns for 30 years or more. With deep wells costing more than a million dollars to drill, it is imperative that the scientific community should plan on long-term observation. Examples of this are the monitoring being planned on the Long Valley Scientific core hole and the San Andreas Observatory at Depth. Plans for monitoring at the Hawaii Scientific Drilling Program (HSDP) hole on Hawaii are in the initial stages. Second, technology is now available to engineer earth observatories with multiple completions having different observational tasks. Deep boreholes provide access to the subsurface, while directional drilling techniques can be used to deploy instrumentation outside the main access well. This allows for the isolation of different instrumentation packages from the influence of the main borehole. We also believe that assemblies similar to core barrels can be used to deliver instrument packages both during and following drilling operations.

In addition to changes in topics and approaches to subsurface science, the technology for drilling is undergoing changes. The commercial drilling industry is often used for the drilling of scientific holes; however, recently specialized drill rigs have been constructed specifically for scientific drilling. These new developments include the DOSECC Hybrid Coring System (DHCS) and the GLAD800 lake coring system.

The DHCS has been used to continuously core the Hawaii Scientific Drilling Program (HSDP) well to a depth of 3109 m and will soon deepen that hole to a projected depth of 4,500 m. This rig uses both oil field and mining technology to improve the efficiency of deep, continuous coring. Mining, or wireline diamond coring, technology is a superior means for the collection of high-quality core samples. This is made possible by the availability of a wide variety of bits for different lithologies that are driven at relatively high speed with low weight on bit. However, there are few mining operations that have a need for sampling at depths greater than 2000 m. Oil-field (and geothermal) drilling technology is designed to drill holes rather than collect samples. Equipment is very good at deep drilling and handling heavy strings of pipe and casing. The DHCS combines these technologies by mounting a top drive and diamond coring package on a rotary drill rig. This technology has been used at a number of geothermal systems throughout the world in addition to scientific drilling.

The GLAD800 system was built to collect long cores from modern lakes. The rig has presently cored The Great Salt Lake, Bear Lake (both in Utah) and Lake Titicaca (Bolivia). Modifications of this system have included using smaller barge and coring rig for drill string lengths of up to 200 m and the development of a heave compensated system for use in the shallow marine environment. In February, our CS-500 drilling rig and lake sampling tools is scheduled to core three lakes in Iceland. For this project, the rig will be mounted on the ice.

Samband skjálftavirkni á Reykjaneshrygg við V-laga hryggi og jarðskorpumyndun

Páll Einarsson og Julia Rohlfs

Háskóla Íslands, Raunvísindadeild

Jarðskjálftavirkni sem fylgir virkum úthafshryggjum er af tveimur megingerðum. Á þver-gengjum stafa skjálftar af sniðgengishreyfingum, stærstu skjálftar fara vel yfir stærðina 6 og b-gildi fyrir stærðardreifingu þeirra er um 1, sem er algengt gildi á skjálftasvæðum heimsins. Á hryggjarstykki, hins vegar, eru skjálftar tengdir siggengishreyfingum, skjálftar verða sjaldan stærri en 5,5 og b-gildi er hátt, oft stærra en 2. Svo há b-gildi eru sjaldgæf nema á eld-virkum svæðum. Almennt gildir að skjálftavirkni er lág á hryggjum með háum rekhraða og há á hægum hryggjum. Skjálftavirkni á Atlantshafshryggnum er þannig fremur há enda er rek-hraði um hann fremur lágur. Frá þessari meginreglu eru þó undantekningar og er skjálfta-virkni á Reykjaneshrygg eitt helsta dæmið um slíkt. Á syðsta hluta Reykjaneshryggjar er skjálftavirknin fremur há og lík því sem gerist sunnar á Atlantshafshryggnum. Hryggurinn snýr hér nánast hornrétt á rekstefnuna, eftir ás hans liggur sigdalur og landslag er hrjúft. Norð-an við 57°N verður hryggurinn mjög skásettur á rekstefnuna og heldur hann þeirri stefnu allt til Íslands. Landslagið á hryggjarásnum er hér líka sléttara og sigdal vantar. Þessi einkenni fylgja annars hryggjum með hærri rekhraða. Skjálftavirknin fylgir þessu líka og er mun lægri en hún er sunnar á hryggnum. Þessi einkenni hafa verið talin stafa af nálægð Reykjanes-hryggjarins við heita reitinn á Íslandi.

Við athuguðum dreifingu skjálftavirkni á Reykjaneshryggnum á tímabilinu 1960-2000 og fengum eftirfarandi niðurstöður:

1. Stærðardreifing skjálftanna hefur b-gildi 2,4.
2. Staðfest er að einungis lítill hluti af rekhreyfingum um flekaskilin kemur fram í misgengishreyfingum og skjálftum, á stærðarþrepi 1 %.
3. Á tveimur svæðum á hryggnum er skjálftavirknin mjög lág eða nánast engin. Þessar skjálftaeyður eru þar sem svokallaðir V-laga hryggir skera hryggjarásinn. V-laga hryggir hafa verið skýrðir með tímabundinni aukningu í virkni Íslandsstróksins sem sendi púlsa af möttulefni suður eftir hryggjarásnum. Giskað hefur verið á að jarðskorpan sem verður til þar sem púlsinn fer um sé um 2 km þykkari en annars staðar. Lág skjálftavirkni á þessum stöðum er því í samræmi við ofangreinda reglu um öfugt samband milli skjálftavirkni og jarðskorpumyndunar.

InSAR observations of crustal deformation in Iceland

Rikke Pedersen¹, Freysteinn Sigmundsson¹, Kurt Feigl², Carolina Pagli^{1,3}, Helene Vadon⁴ and Erik Sturkell⁵.

¹Nordic Volcanological Institute, Iceland; ²CNRS, France; ³Science Institute, University of Iceland.; ⁴CNES, France; ⁵Icelandic Meteorological Institute, Iceland

In Iceland different sources of deformation in a variety of tectonic settings have been detected by Interferometric combination of Radar Satellite Images (InSAR). Among these are:

- 1): Intrusions in the Eyjafjallajökull area. Images spanning 1993-2000 identify considerable surface deformation, with 5 concentric fringes visible in the area south of the Eyjafjallajökull icecap. The deformation has also been detected by tilt and GPS campaign measurements, as well as high seismic activity.
- 2): Earthquake faulting in the SISZ and on the Reykjanes Peninsula, due to the seismic activity in June 2000 is detected in several images. On June 17, and June 21, 2000 two M_s 6.6 earthquakes ruptured N-S striking faults in the SISZ. Joint inversion of InSAR and GPS data indicates that the two events ruptured faults 15 km long extending to about 9 km depth. Maximum slip, reaching more than 2 meters in both events, is concentrated in the upper crust, from the surface to 5-6 km depth. Dynamic triggering of earthquakes on the Reykjanes Peninsula followed the June 17, 2000 M_s 6.6 earthquake in the SISZ, about 80 km to the east of the main event. Inverse modeling of the InSAR data estimates the deformation to originate from a M_w 5.8 and a M_w 5.3 events, when assuming uniform slip on two simple rectangular fault patches.
- 3): An eruption at Hekla volcano began on February 26, 2000. Short-term precursory seismic activity was detected about one hour before the eruption started. Initially, a 6-7 km long eruptive fissure opened up along most of the Hekla ridge. Deformation due to the eruption is seen in a series of interferograms. The displacements appear to be the results of dike opening as well as subsidence due to deflation of a deep-seated magma chamber.
- 4): Surface inflation due to inflow of magma in the Hengill area can be seen in images spanning 1993 to 1998. The uplift signal can be explained by an expanding Mogi-source at 7 km depth, with 2-cm/year inflation rate. Persistent seismicity during 1994 to 1998 was associated with the widespread uplift.
- 5): Long-term subsidence in the Askja caldera has now been recognized not only by tilt and GPS, but also in InSAR images. A small, but obvious subsidence signal amounting to 1 fringe is seen in the Askja caldera in an image spanning 1998-1999. Other images spanning longer periods show larger deformation signals. The size of the deformation scales well with the time span of the images. The subsidence can be partly related to cooling of a magma chamber.
- 6): Readjustment of the spreading segment at Krafla has been detected in InSAR images spanning 1992 to 1996. Most deformation occurs above an inferred shallow magma chamber, which fed events during the 1975 to 1984 rifting period. The subsidence is elongated along the spreading axis, which is interpreted to be due to cooling contraction and ductile flow of material away from the spreading axis.

Ion hydration and isotope fractionation in hydrothermal solutions

T.M. Seward, ETH Zürich

The stable isotopes of oxygen and hydrogen have long been used as versatile and powerful geochemical probes for the study of fluid-rock interaction processes. The reconstruction of paleotemperatures, fluid sources and fluxes and the localisation of fluid pathways can in principle, be quantitatively considered using stable isotope methods. However, a fundamental requirement for any meaningful application of such isotope methods is an accurate knowledge of the fractionation factors for the relevant mineral-fluid exchange equilibria involved.

A number of recent studies (e.g. Horita et al, 1995, Driesner and Seward, 2000) have shown that the fractionation factors for isotope exchange reactions involving water may change considerably in the presence of dissolved salts as temperature and pressure change from ambient to hydrothermal conditions. For example, in the case of alkali metal chloride solutions (e.g. 4.0m NaCl and KCl), a difference of more than one per mil in the $^{18}\text{O}/^{16}\text{O}$ liquid-vapour fractionation in comparison with pure water occurs with increasing temperature up to 380°C.

Thus, electrolyte solutions in equilibrium with water vapour become isotopically heavier with respect to pure liquid water as H_2^{18}O and HDO fractionate in the hydration shells around ions at elevated temperature. These isotope salt effects arise predominantly from molecular interactions affecting the water molecules in the first hydration shell of ions. Classic thermodynamic approaches together with quantum chemical and molecular dynamics computations and simulations provide considerable insight into the nature of the isotope salt effect. In particular, changes in the internal intramolecular vibrational modes of first shell water molecules induced by an ion charge field are most important whereas, rotational and translational contributions are small in most systems of geochemical interest.

Configurational changes attending ion hydration as a function of temperature and pressure are also intimately associated with isotope salt effects. We have therefore been studying ion hydration in aqueous solutions over a range of temperatures from 25 to 360°C using X-ray absorption spectroscopy (i.e. Exafs) in order to measure changes in the hydration environments of ions with respect to ion-oxygen (water) distances and the changes in the number of coordinated water molecules. Measurements have been conducted at the Daresbury (UK) and ESRF (Grenoble) synchrotron facilities using high temperature-high pressure, X-ray optical cells containing silica and diamond windows. In the case of the Ag^+ ion, for example, the first shell waters are tetrahedrally coordinated at 25°C at a distance of 2.32Å. With increasing temperature to 350°C at saturated vapour pressures, the number of first shell waters decreases to three and the silver-oxygen (water) distance decreases to 2.22Å (Seward et al, 1996). In the case of an anion such as iodide (Seward et al, 2003), the ion is surrounded by seven water molecules at a distance of 3.55Å. With increasing temperature to 350°C, the number of coordinated waters decreases from seven to four as the iodide-oxygen (water) distance increases to 3.63Å. These temperature induced contractions and/or expansions of the first hydration shell waters around ions have also been confirmed using high temperature uv spectroscopy and ab initio/molecular dynamics simulations. These configurational changes play a fundamental role in defining isotope salt effects and it may be shown, for example, that small changes in the ion-water distance can cause significant changes in the asymmetric stretching frequency of a water molecule in the field of ions. Further studies are in progress.

Driesner T. and Seward T.M. (2000) *Geochim. Cosmochim. Acta* 64, 1773.

Horita J., Cole D.R. and Wesolowski D.J. (1995) *Geochim. Cosmochim. Acta* 59, 1139.

Seward T.M., Henderson C.M.B., Charnock J.M. and Dobson B.R. (1996) *Geochim. Cosmochim. Acta* 60, 2273.

Seward T.M., Henderson C.M.B., Charnock J.M. and Suleimenov O.M. (2003) *Geochim. Cosmochim. Acta* 67 (in press).

The tephra layer from the 1362 Öräfajökull eruption, SE-Iceland: A Plinian eruption associated with a caldera collapse

Rune S. Selbekk

Nordic Vulcanological institute, University of Iceland, Grensásvegur 50, IS-108 Reykjavik, *E-mail:* rune@norvol.hi.is *Tel:* +354-525-5482, *Fax.:* +354-562-9767

Pyroclastic fallout from the 1362 eruption of Öräfajökull forms one of the volcanic marker horizons of the North Atlantic. This contribution reports the mineralogical and geochemical characteristics of the Öräfajökull 1362 fallout and its grain-size distribution. A non-rifting 120 km long volcanic lineament some 50 km east of the Eastern Rift-Zone of Iceland is defined by transitional and alkalic volcanic rocks resting unconformably on late Tertiary strata. Öräfajökull which forms the southern termination of this off-rift liniment is an ice-covered stratovolcano (2200 masl) composed mostly of subglacially formed hyaloclastite ranging from basalts to rhyolites. The two historical (1100 yrs) eruptions of Öräfajökull include a small explosive eruption in 1727 and a large devastating Plinian eruption associated with major lahars and a caldera collapse in 1362. Between 1 and 2 km³ dense rock equivalent or 5-10 km³ of rhyolitic pumice was erupted and the fallout was mainly towards ESE. Tentative modelling of the PT-conditions of the magma formation, based on glass/mineral equilibria, indicates that the source was a near-eutectic melt in equilibrium with fayalite, hedenbergite, oligoclase and hematite at some 0.2 GPa pressure.

A profile through the fallout was sampled at elevation of about 1100 masl on the SE flank of the volcano. A deposit of 1.8 m thickness was collected in 14 units for examination of composition, mineralogy and grain-size distribution during the eruption. In the profile the fallout is fine grained vesicular glass (1-3% minerals, 3% lithic fragments) with bubble wall thickness in the low micron range. The high and even vesiculation of the glass indicates fast magma ascent and explains the extreme mechanical fragmentation within the eruptive column, yielding between 50 and 80 wt% of less than 0.25 mm grain size.

A reconstruction of the Plinian phase, based on grain-size analysis and abundance of lithic fragments, reveals that the eruption proceeded in three successive phases. An initial explosion produced phreatomagmatic debris associated with up to 35% of lithic fragments. In distal facies of the fallout, the initial phase is recognised as pale brownish base of the otherwise white glassy layer. The material ejection proceeded in two largely similar phases. These phases are separated only by a transition in grain size distribution indicating a temporary lowering in the effusion rate.

The surface of the fallout is characterised by increasing pumice dimensions and occasional bomb-like pumice blocks indicating less mechanical fragmentation during contraction and lowering of the Plinian column. The eruptive phases represent a tectonic events associated with a caldera collapse mechanism of the eruption since they are only displayed in the grain size distribution of the otherwise homogeneous material.

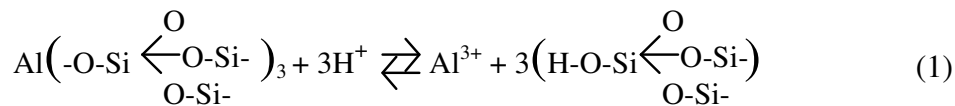
Basaltic Glass Dissolution

Sigurður R. Gíslason¹, Eric H. Oelkers²,; Domenik Wolff-Boenisch¹ and Ólafur Arnalds³,

¹Science Institute, University of Iceland, Dunhagi 3, 107 Reykjavík, Iceland, sigr@raunvis.hi.is; ²Géochimie: Transferts et Mécanismes, CNRS/URM 5563--Université Paul Sabatier, 38 rue des Trente-six Ponts, 31400 Toulouse, France, oelkers@lmtg.ups-tlse.fr; ³Science Institute, University of Iceland, Dunhagi 3, 107 Reykjavík, Iceland, boenisch@hi.is, ³Agricultural Research Institute, Reykjavík, Iceland, ola@rala.is.

The rapid cooling of magma produces about a billion cubic meters (1 km³) of glass each year, mainly along the 70,000-km oceanic ridge system (Morgan and Spera, 2001). Most of this glass is of basaltic composition. According to Nesbitt and Young (1984) volcanic glass is about 12.5% of the average exposed continental crust surface. Of the average upper continental crust minerals, only plagioclase feldspar (34.9%) and quartz (20.3%) are more abundant. Owing to its volume and relatively high reactivity, basaltic glass dissolution plays a critical role in the global cycling of a significant number of elements and of CO₂.

Towards the quantification of the role of basaltic glass in surficial processes, we have experimentally measured the dissolution rates of a variety of natural glasses as function of temperature, glass surface area, and aqueous solution composition, including pH and the aqueous concentrations of Si, Al, F, and organic anions. All of these data are consistent with the assumption that basaltic glass dissolution rates are controlled by the concentration of Si atoms bridged by two bridging oxygens (Si^{II}) at the basaltic glass surface (see Oelkers, 2001). The two major sources of Si^{II} are 1) Si atoms at glass edges and 2) Si atoms adjoining previously exchanged trivalent metals; the exchange of aluminium for three protons at the surface leads to the formation of three partially liberated Si^{II} atoms in accord with



Assuming that the number of Si^{II} atoms formed from this aluminium exchange reaction is far in excess of those present at glass edges, which appears to be the case at steady state dissolution (Oelkers and Gíslason, 2001; Gíslason and Oelkers 2002), the overall forward or ‘far from equilibrium’ basaltic glass dissolution rate when there is a significant Al concentration at the near surface, can be described using (Oelkers and Gíslason, 2001; Gíslason and Oelkers 2002),

$$r_{+,geo} = A_A \exp^{-\left(\frac{E_A}{RT}\right)} \left(\frac{a_{\text{H}^+}^3}{a_{\text{Al}^{3+}}}\right)^{0.33} \quad (2)$$

where $r_{+,geo}$ signifies the geometric surface area normalised far from equilibrium steady state basaltic glass dissolution rate, A_A refers to a constant, E_A designates an apparent activation energy, R stands for the gas constant, T signifies temperature in °K, and a_i represents the activity of the subscripted aqueous species. Computed values of BET surface area normalised ‘far from equilibrium’ steady state basaltic glass dissolution rates in 0.1 molal ionic strength solutions containing 10⁻⁶ mol/kg Al and void of Al complexing aqueous species other than OH⁻ are illustrated as a function of pH at various temperatures in Fig. 1. This figure was created in terms of B.E.T. normalised surface areas to allow their comparison with B.E.T. surface area normalised dissolution rates of other minerals available in the literature.

Oelkers and Gíslason (2001) found the affect of aqueous oxalate on the dissolution rate of basaltic glass to stem from its affect on aqueous aluminium activity. Therefore, it seems likely that the affect of other aqueous Al complexing anions, such as other organic acid anions, fluoride, or silica on basaltic glass dissolution rates can be successfully estimated using Eqn. (2) together with aqueous aluminium activities determined from solute speciation calculations. The pH dependence of 25° C steady state far from equilibrium basaltic glass dissolution rates at various oxalate, acetate, fluoride or silica ion concentrations are illustrated in Figs. 2 to 5. Note that these anions will not only affect the dissolution rate of basaltic glass, but also the solubility of Al bearing primary and secondary minerals, and therefore the overall mobility of elements contained in these phases during water-rock interaction.

Calculated values of basaltic glass dissolution rates as a function of pH in the presence of aqueous oxalate and acetate concentration are illustrated in Figs. 2-3. These anions have little affect on basaltic glass dissolution rates at the pH of typical river or ocean waters (pH 7-8). In contrast, in soil, where the pH is lower (pH 4-7), organic acid basaltic glass dissolution rate enhancement is greatest. It follows that the secretion of organic acids by terrestrial plants will be most efficient in releasing nutrients such as Ca, Mg, K, Fe, and P from basaltic glass at the pH's typical of terrestrial soil solutions. The more organic acid a given plant and its associated micro-organism is able to secrete, the better it is equipped to compete for basaltic glass derived nutrients. This finding is in concert with microscopic and macroscopic measured enhancement of natural chemical weathering rate of basalt in bare versus vegetated areas. (Gíslason et al. 1996; Berner and Cochran 1998; Moulton and Berner 1998; Stefánsson and Gíslason 2001).

The effect of aqueous silica concentration on basaltic glass dissolution rates, at a constant Al total concentration of 10^{-6} M, is shown in Fig. 4. There will be some effect of aqueous Si on these rates in the pH range typical of ocean, lake, river and ground waters (pH 7-10). According to Fig. 4, primary production in surface waters will enhance the dissolution rate by increasing pH, but the magnitude of the effect depends on the primary producer. Per pH change, diatoms have less effect than algae that do not fix silica. Primary production by diatoms both results in increasing pH and a decrease in total silica concentration of surface waters, resulting in relatively little dissolution enhancement.

The effect of aqueous fluoride concentration on basaltic glass dissolution rates is shown in Fig. 5. Of the anions considered in this study, fluoride has the greatest effect on rates at pH < 8. This observation has numerous consequences concerning the mobility of elements in volcanic terrain during water-rock interaction (Wolff-Boenisch and Gíslason 2002). The concentration of fluoride in Icelandic rivers, from west to east, across the mid-Atlantic ridge range from 0.02 to 0.7 ppm, reaching highest concentration in the middle of the rift zone. The concentration in ground waters and geothermal waters in Iceland range from 0.02 to few ppm, and the concentration variation in melted snow in contact with pristine volcanic ash is from less than one ppm to more than 200 ppm. This fluoride concentration variation should result in enormous dissolution rate variation. The concentration of total dissolved solids versus fluoride concentration in the springs in the vicinity of Mt Hekla volcano, Iceland is shown in Fig. 6. The higher the F, the higher the TDS concentration. One order of magnitude increase in fluoride concentration results in a one order of magnitude increase in total dissolved solids. Because of the high aqueous F concentration and relative low pH, basaltic glass dissolution is expected to be most aggressive within the rift zones of the oceanic ridges.

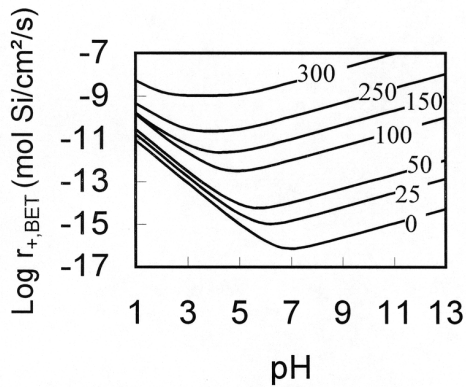


Figure 1. Basaltic glass dissolution rates in solutions containing 10^{-6} mol/kg Al and void of Al complexing aqueous species other than OH^- . Figures 1 to 5 were calculated by (Eqn. 2) in terms of B.E.T. normalised surface areas using a roughness factor of 92.

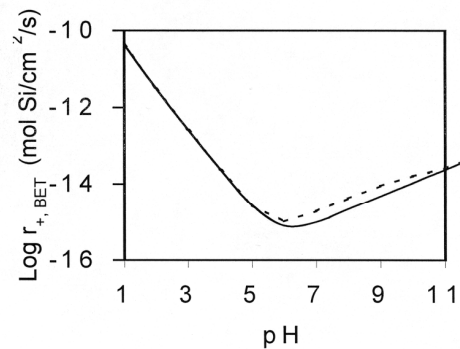


Figure 4. Basaltic glass dissolution rates at 25 °C in solutions containing 10^{-6} mol/kg Al and a) void of Al complexing aqueous species other than OH^- , b) the upper curve, 1 mmol/kg total dissolved Si.

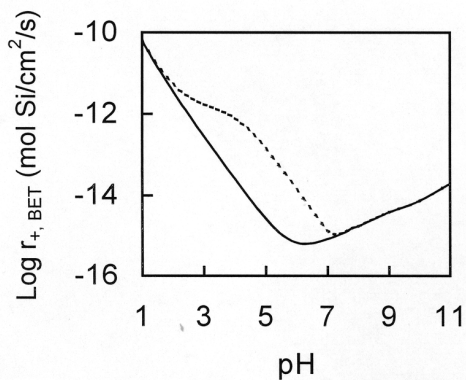


Figure 2. Basaltic glass dissolution rates at 25 °C in solutions containing 10^{-6} mol/kg Al and a) void of Al complexing aqueous species other than OH^- , b) the upper curve, 1 mmol/kg oxalate.

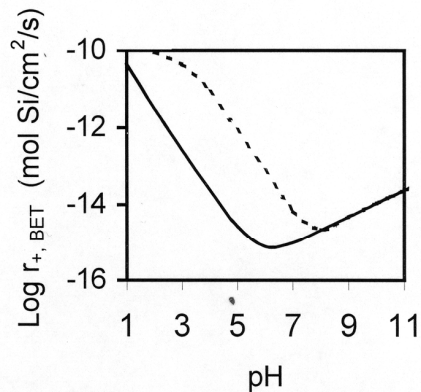


Figure 5. Basaltic glass dissolution rates at 25 °C in solutions containing 10^{-6} mol/kg Al and a) void of Al complexing aqueous species other than OH^- , b) the upper curve, 1 mmol/kg total dissolved F.

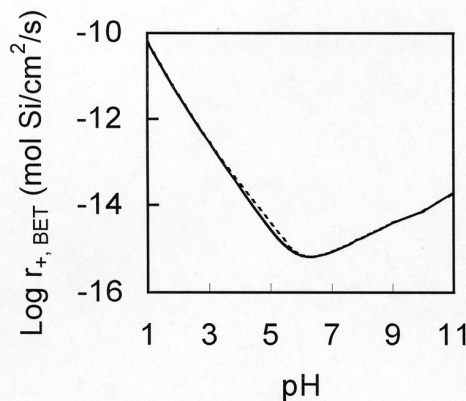


Figure 3. Basaltic glass dissolution rates at 25 °C in solutions containing 10^{-6} mol/kg Al and a) void of Al complexing aqueous species other than OH^- , b) the upper curve, 1 mmol/kg acetate.

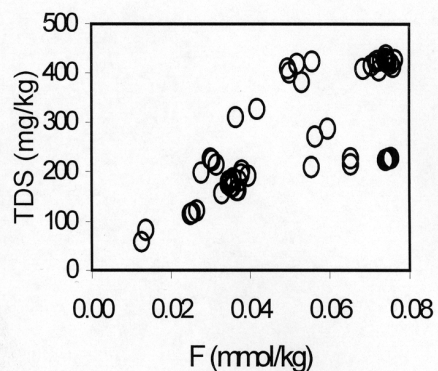


Figure 6. The concentration of total dissolved solids versus fluoride concentration in the springs (2-4.5 °C) in the vicinity of Mt Hekla volcano, Iceland.

References

- Berner R. A. and Cochran M. F. (1998). Plant-induced weathering of Hawaiian basalts. *Journal of Sedimentary Research* 68, 723-726.
- Gíslason S. R. and Oelkers, H.E. (2002). The mechanism, rates and consequences of basaltic glass dissolution: II. An experimental study of the dissolution rates of basaltic glass as a function of pH at temperatures from 6°C to 150 °C. *Geochimica et Cosmochimica Acta* (submitted).
- Gíslason, S. R., Arnórsson, S., and Ármannsson, H. (1996). Chemical weathering of basalt in SW Iceland: Effects of runoff, age of rocks and vegetative/glacial cover. *American Journal of Science*, 296, 837-907.
- Morgan, N.A. and Spera, F.J. (2001). Glass transition, structural relaxation, and theories of viscosity: A molecular dynamics study of amorphous $\text{CaAl}_2\text{Si}_2\text{O}_8$. *Geochimica et Cosmochimica Acta* 65, 4019-4041.
- Moulton, K.L, West, J., and Berner, R.A. (2000). Solute flux and mineral mass balance approaches to the quantification of plant effects on silicate weathering. *American Journal of Science* 300, 539-570.
- Nesbitt, H. W. and Young, G. M. (1984). Prediction of some weathering trends of plutonic and volcanic rocks based on thermodynamic and kinetic considerations. *Geochimica et Cosmochimica Acta* 48, 1523-1534.
- Oelkers, H.E. (2001). General kinetic description of multioxide silicate mineral and glass dissolution. *Geochimica et Cosmochimica Acta* 65, 3703-3719.
- Oelkers, H.E. and Gíslason, S. R. (2001). The mechanism, rates and consequences of basaltic glass dissolution: I. An experimental study of the dissolution rates of basaltic glass as a function of aqueous Al, Si, and oxalic acid concentration at 25°C and pH 3 and 11. *Geochimica et Cosmochimica Acta* 65, 3671-3681.
- Stefánsson, A. and Gíslason S. R. (2001). Chemical weathering of basalts, SW Iceland: effect of rock crystallinity and secondary minerals on chemical fluxes to the ocean. *American Journal of Science* 301, 513-556.
- Wolff-Boenisch, D. and Gíslason, S.R (2002). Dissolution rate of volcanic glass as a function of glass composition. Abstract Volume, The 25th Nordic Geological Winter Meeting, January 6th – 9th, 2002, Reykjavík, Iceland. p. 232.

Gler-innlyksur í kristöllum úr Búrfells-pikríti í Ölfusi

Sigurður Steinþórsson¹ og Ingvar A. Sigurðsson²

¹Raunvísindastofnun Háskólans, ²Náttúrustofa Suðurlands, Vestmannaeyjum

Efnasamsetning gler-innlyksa í króm-spínli og ólivíni úr pikrítmyndun Búrfelli í Ölfusi myndar samfellda röð sem í MgO-styrk spannar 13,6 til 8,4 þunga%. Krómít-innlyksurnar eru MgO-ríkari en innlyksur ólivínsins og hóparnir tveir skarast óverulega: í krómíti er MgO > 11% en í ólivíni er MgO < 11%. Þegar efnagreiningunum er varpað í kerfið ol'-ne'-q', sem Takahashi og Kushiro (1983) kvörðuðu með jafnþrýstilínunum fyrir bráðir í jafnvægi við möttulsteindir, kemur í ljós að innlyksurnar spanna þrýstibilið 17 til 7 kb, samsvarandi 50 til 20 km dýpi. Gild rök eru fyrir því að innlyksurnar hafi lokast inni í kristöllum — einkum króm-spínli — mjög fljótlega eftir að bráðin myndaðist, því í Borgarhrauni hjá Þeistareykjum má greina tvær óskyldar kvikuraðir í innlyksum, sem sýna engin merki blöndunar (Ingvar A. Sigurðsson et al. 2001). Hér er því um að ræða frumbráðir sem mynduðust við bráðun á mismunandi dýpi undir Íslandi.

Ólíkt efnum eins og Al₂O₃, CaO, FeO og TiO₂ sem breytast kerfisbundið með MgO, eru engin sýnileg vensl milli styrks MgO og utangarðsefnisins K₂O sem spannar 0,01 - 0,05%. Þennan fimmfalda mun í K₂O mætti skýra á tvo vegu, (1) sem afleiðingu samfelldrar hlutbráðunar sama móðurefnis og (2) sem blöndur tveggja kvika, K-ríkrar og K-snauðrar. Ef um samfellda uppbræðslu væri að ræða, ætti frumstæðasta, MgO-ríkasta bráðin jafnframt að vera hin K₂O-ríkasta og hafa myndast við hæsta mældan og reiknaðan hita, en hvorugu er að heilsa. Samkvæmt þessu er síðara líkanið sennilegra, í samræmi við þá niðurstöðu Gurenko & Chaussidon (1995) að undir Reykjanesskaga séu tvær kvikur, „sneydd“ (depleted) og „auðguð“ (enriched). Allar innlyksur, sem greindar voru úr Búrfelli, tilheyra „sneydda“ hópnum.

Á vörpun K₂O/TiO₂ vs. K₂O mynda spinel-innlyksurnar beina línu sem túlka má sem frumbráðir, meðan samsetning ólivín-innlyksanna bendir til dálítillar þróunar frá frumbráð. Gögnin má túlka þannig að spínil-innlyksurnar hafi myndast yfir mestan hluta þrýstibilsins (17-7 kb) við bráðun spínil-lherzólíts þar sem klínópýroxen er stærsti þáttur bráðarinnar, en ólivín-innlyksurnar hafi einkum myndast í kvikuhólfi á 20 km dýpi (7-8 kb) þar sem ólivín og plagíóklas kristölluðust.

Tilvísanir

Gurenko A.A. and Chaussidon M., (1995). *Geochim. Cosmochim. Acta* 59, 2905-1917.

Sigurðsson I.A., Steinthorsson S. and Grönvold K., (2000). *Earth Planet. Sci. Letters* 183, 15-26.

Takahashi E., Kushiro I., (1983). *Am.Mineral.* 68, 859-879.

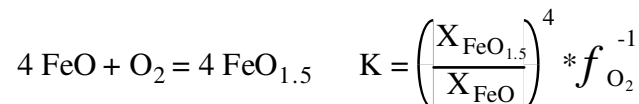
Oxunarstig basaltbráðar sem fall af ildisprýstingi, hitastigi og efnasamsetningu

Sigurður Steinþórsson og Örn Helgason

Raunvísindastofnun Háskólans

Oxunarstig bergkviku, Fe(III) / Fe(II), er mikilvægur eiginleiki sem miklu veldur um samsetningu og hlutföll þeirra steinda sem kristallast, og þar með um þróun bráðar við kólnun og kristöllum. Ferró/ferrí-hlutfallið verður að mæla sérstaklega, því hvorki örgreinir né aðrar röntgen-aðferðir greina milli þriggils og tvíggils járns. Tilgangur þessa rannsóknaverkefnis var að tengja með bergfræðitilraunum Fe^{3+}/Fe^{2+} -hlutfall, ildisprýsting (fO_2), hita (T) og efnasamsetningu basalts, bæði með það fyrir augum að öðlast skilning á oxunarferlinu, og að útleiða jöfnur sem lýsa ofangreindum venslum.

Fjögur sýni voru valin sem spanna efnasamsetningu basalts á Íslandi, frá ólivín-þóleiíti til ne-normalífs alkalíbasalts. Sýnin voru brædd við $1300^\circ C$ og mismunandi fO_2 milli 1 og 10^{-9} atm, og ferrí/ferró-hlutfallið síðan mælt með Mössbauer-tækni. Allt frá 5. áratug 20. aldar, þegar Kennedy (1948) gerði fyrstu tilraunirnar í þessa veru, hefur verið talið að línulegt samband ríki milli fO_2 og Fe^{3+}/Fe^{2+} , t.d.



$$\log \left(\frac{X_{FeO_{1.5}}}{X_{FeO}} \right) = \frac{1}{4} \log f_{O_2} + \frac{1}{4} \log K$$

Nýrri mælingar taka styrk annarra efna inn í jöfnurnar, t.d. Kress & Carmichael (1991):

$$\ln \left(\frac{X_{Fe_2O_3}^{liq}}{X_{FeO}^{liq}} \right) = a \ln f_{O_2} + \frac{b}{T} + c + \sum_i d_i X_i$$

þar sem a, b, c og d_i eru fastar, hinn síðastnefndi mismunandi eftir frumefnum i .

Megin-niðurstöður okkar eru þær að ofangreint samband sé ekki línulegt fyrir allt svið fO_2 , og að samsetning (t.d. styrkur alkalímalma) hafi ekki mælanleg áhrif á ferrí/ferró-hlutfallið. Hins vegar er hinn jarðfræðilega-mikilvægi hluti ferilsins ($fO_2 < 10^{-2}$ atm) nálægt því að vera línulegur svo sem lýst er með jöfnum, t.d. Kress & Carmichael (1991). Ástæðuna fyrir því að oxunarferillinn er ólínulegur er að finna í mismunandi hegðun Fe^{3+} í oxaðri og afoxaðri bráð. Sú tilgáta var staðfest með beinum há-orku röntgenmælingum (EXAFS) sem gerðar voru í Hamborg á þremur sýnum sem spönnuðu oxunarsvið tilraunanna.

Könnun á hraða oxunar-afoxunarhvarfa sýndi að (a) ferlið er jafnhverft, (b) 100 mg sýni nær jafnvægi við sérhvert fO_2 á 4 klst., og (c) hraðkælt náttúrulegt berg, svo sem basaltgler, geymir oxunarstig bergkvikunnar sjálfrar.

Tilvitnanir

Kennedy, G.C. (1948), *American Journal of Science* 246, 529-549.

Kress, V. C. and Carmichael, I.S.E. (1991), *Contrib. Mineral. Petrol.* 108, 82-92.

Low-frequency earthquakes at the Torfajökull volcano, measured by a local network

Heidi Soosalu¹ and Páll Einarsson²

¹Norræna eldfjallastöðin, ²Raunvísindastofnun Háskólans

The Torfajökull central volcano in south Iceland is a large rhyolitic complex with a caldera, 12 km in diameter, and an outstanding high-temperature geothermal field. During the last 1100 years there have been two eruptions in the Torfajökull area, the latest at the end of the 15th century. Torfajökull is a source of continuous low-level seismicity, and the events fall into two distinct populations. Before the operation of our Torfajökull temporary network these events have been detected and located using the permanent SIL network of the Icelandic Meteorological Office and analog seismometers in the vicinity.

High frequency, normal-looking earthquakes occur in the western part of the caldera and are interpreted to be the expressions of thermal cracking around a cooling magma chamber. Low frequency volcanic earthquakes cluster in the southern part of the caldera and are possibly related to active magma. They are small in size, below magnitude 2, and it is quite difficult to obtain good locations for them. Their P-waves are characteristically emergent. The S-waves are often clearer and their phase picks seem to fit more or less with the location. The low frequency events can occur in swarms, lasting from one to a few days and consisting of up to a couple of hundred events per day. Typically the seismicity rises from rather low levels to its highest peak in a single day. Between the swarms there can be occasional single events, or it can be quiet up to a few weeks or months.

A temporary network of 18 intermediate band (30 sec – 50 Hz) 3-component Güralp 6TD seismometers was deployed in the Torfajökull area in the summer 2002 to study more closely the low frequency earthquakes. This sort of activity has been rather modest during the operation of the network, no distinct swarms have occurred so far. However, the activity appears to be constant, as single small low frequency events have been recorded almost daily. Many of these events are too small to be detected by the regional SIL network.

According to the preliminary analysis the recorded events have very similar appearance to those observed earlier by the more distant seismograph stations of the SIL network. The P-arrivals seem very small and emergent, and in most cases only the S-arrival can be picked reliably. These events consist of only low frequencies (about 1-5 Hz), also when seen by stations close by. The first preliminary locations we made are in the middle and southern parts of the Torfajökull caldera, similar to what was observed before.

Primary basalt mineral saturation in surface- and up to 90°C ground waters in Skagafjörður, N-Iceland

Stefán Arnórsson, Andri Stefánsson and Ingvi Gunnarsson

Science Institute, University of Iceland, Dunhagi 3, 107 Reykjavík, Iceland.

INTRODUCTION

This contribution describes the state of primary basalt mineral saturation in surface- and up to 90°C ground waters in the Mid-Tertiary tholeiite flood basalt area of Skagafjörður in central north Iceland. It is based on analysis of 253 samples of surface- and ground waters collected from the area in 1996-98.

GEOLOGY AND HYDROGEOLOGY

The Skagafjörður Valley area in N-Iceland dissects a monotonous pile of 9-12 million year old, slightly quartz to slightly olivine normative, flood basalts. To the south of the Skagafjörður valley system, in the interior highlands, Quaternary formations overlie the Tertiary formations. The total thickness of the succession is about 7 km (Jóhannesson, 1991).

A zone of recent fracturing extends N15°E from the active volcanic belt in central Iceland across the central part of the Valley of Skagafjörður. In several places these fractures are seen to run through ground moraines resting upon the bedrock indicating movement in Post-glacial times. Thermal springs (up to 90°C), which are abundant in the area, are concentrated where the recent fracture zone cuts across the Skagafjörður Valley (Arnórsson and Gíslason, 1990) indicating that the young faults and fractures represent permeability anomalies. Global permeability of the unfractured bedrock below the Skagafjörður Valley floor is considered to be in the range of 10^{-16} to 10^{-14} m² (see Arnórsson et al., 2002). In rocks forming the higher mountains on either side of the valley and the interior plateau to the south of the Skagafjörður valley system and north of the icecap of Hofsjökull, permeability will be higher, probably by one to two orders of magnitude as deduced from data presented by Saemundsson and Fridleifsson (1980) on drillholes sunk into Tertiary and Quaternary basalts in Iceland. From the inferred global permeability in the Skagafjörður area, assuming that the hydraulic gradient follows the topography, it is estimated that water emerging in springs in the Valley of Skagafjörður may be thousands of years old, whereas spring waters in the interior plateau are probably at the most a few decades old.

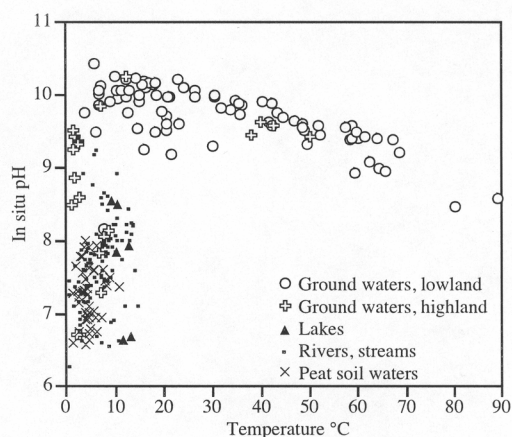


Fig. 1 In situ pH versus temperature of waters from Skagafjörður.

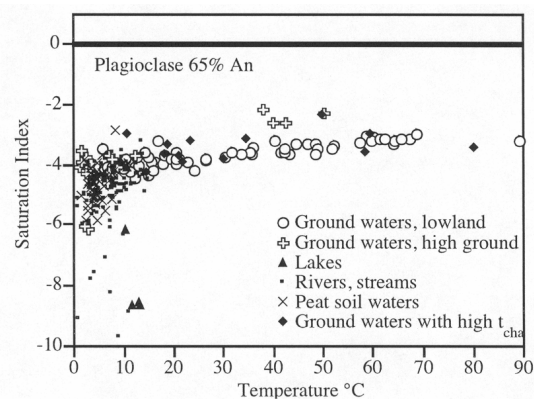


Fig. 2. Temperature versus saturation index for plagioclase, of average composition (An = 0.65).

WATER COMPOSITIONS

The sampled waters have been divided into five groups on the basis of the geological/hydrological environment they occur in as (1) stream- and river waters, (2) lakes, (3) peat soil waters, (4) ground waters on high ground and (5) ground waters on low ground. The ground waters are both thermal and non-thermal. The reason for splitting the ground waters into two groups is based on the inferred permeability of the enclosing rock and, therefore, their residence time underground (Arnórsson et al., 2002). The residence time of the ground waters is expected to affect the amount of water-rock interaction and, in this way, their chemistry.

All water types from the study area are low in total dissolved solids, 7-430 ppm. The dissolved solids content of the ground waters increases with temperature, largely due to an increase in Si, Na and SO₄ concentrations but to a lesser extent by an increase in Cl concentrations. Waters associated with peat soil, which is rich in organic matter, are generally higher in dissolved solids than stream and river waters.

The in situ pH of the waters, as calculated by the WATCH speciation program (Arnórsson et al., 1982), version 2.1A (Bjarnason, 1994), relates to the environment in which they occur. Almost all ground waters have a high pH, in the range 9-10 (Fig. 1). By contrast, waters from streams, rivers and lakes have a lower pH value, typically 7.5 to 8.5 but the peat soil waters tend to have the lowest pH. According to Arnórsson et al. (1995), the pH of both surface- and ground waters in Iceland is the consequence of three processes, (1) dissolution of the mafic minerals and glass, (2) supply of acids to the water and (3) precipitation of OH-bearing minerals. The first process increases the pH whereas the latter two tend to lower it.

PRIMARY BASALT MINERAL SATURATION

Surface waters are significantly under-saturated with plagioclase and olivine of the compositions occurring in the study area, saturation index (SI) values ranging from -1 to -10 and -5 to -20, respectively. With few exceptions these waters are also significantly under-saturated with pigeonite and augite of all compositions (SI = -1 to -7) and with ilmenite (SI = -0.5 to -6). The surface waters are generally over-saturated with respect to the titanomagnetite of the compositions occurring in the basalts of the study area, the range in SI being from -2 to +10. Stabilization of the titanomagnetite is considered to result from oxidation of ferrous iron leached from the mafic minerals. For crystalline OH-apatite, SI-values range from strong under-saturation (-10) to strong over-saturation (+5) but for crystalline F-apatite the SI-values lie in the range 0-15. Systematic under-saturation is, on the other hand, observed for "amorphous apatite", i.e. an apatite of the kind Clark (1955) prepared by mixing Ca(OH)₂ and H₃PO₄ solutions.

Ground waters are under-saturated with plagioclase and olivine, its degree increasing with increasing Ca content of the plagioclase and increasing Fe content of the olivine, the SI values being -2 to -7 and 0 to -4 for the Ca-richest and Ca-poorest plagioclase, respectively, and about -3 to -18 and 0 to -15 for forsterite and fayalite, respectively. Ground waters are generally close to saturation with pigeonite and augite of all compositions. Above 25°C the ground waters are ilmenite under-saturated but generally over-saturated at lower temperatures. These waters are titanomagnetite over-saturated at temperatures below 70°C, the SI values decreasing with increasing temperature from about 6-8 at 10°C to 0 at 70°C. The ground waters are highly over-saturated with both crystalline OH- and F-apatite but close to saturation with "amorphous apatite" containing about equal amounts of F and OH.

The above described results for the pyroxenes carry an unknown error because available thermodynamic data do not permit but a simple solid solution model for the calculation of

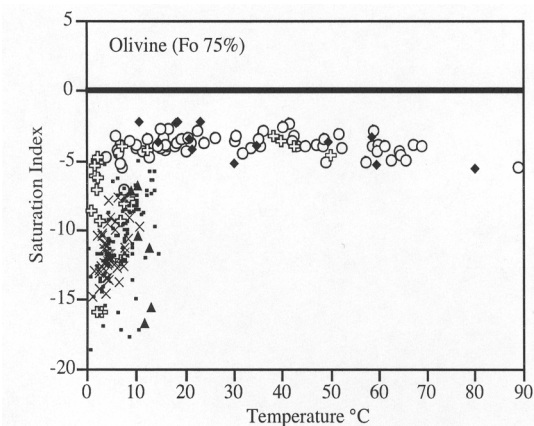


Fig. 3. Temperature versus saturation index for olivine of average composition (Fo = 0.75). Symbols refer to legend on Fig. 2.

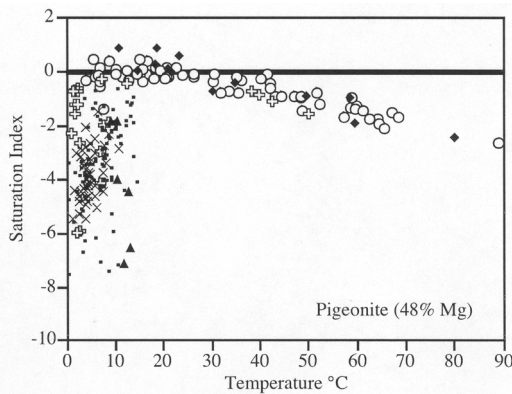


Fig. 4. Saturation index for pigeonite of average composition (Mg = 0.48). Symbols refer to legend on Fig. 2.

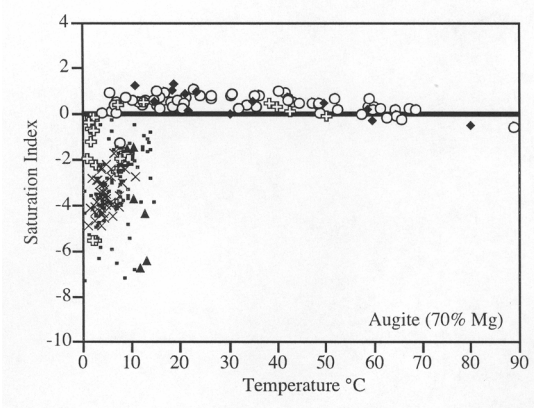


Fig. 5. Temperature versus saturation index for augite of average composition (Mg = 0.7). The symbols refer to legend on Fig. 2

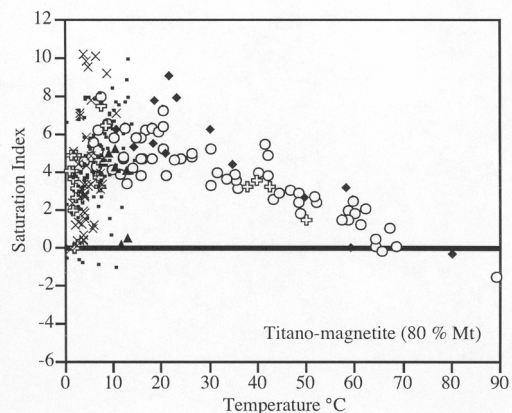


Fig. 6. Saturation index for titano-magnetite of average composition (Mt = 0.8) as a function of temperature. Symbols refer to legend on Fig. 2.

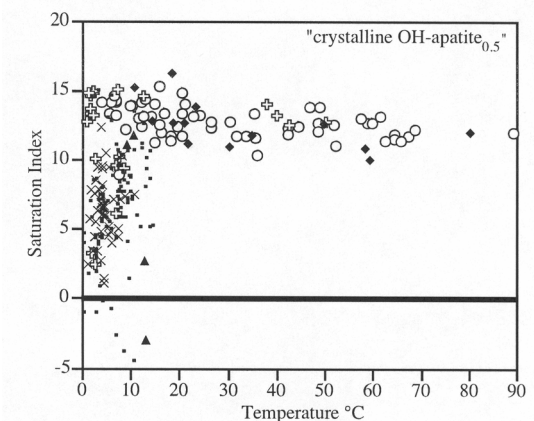


Fig. 7. Saturation index for crystalline apatite containing equal amounts of OH and F and as a function of temperature. Symbols refer to legend 2.

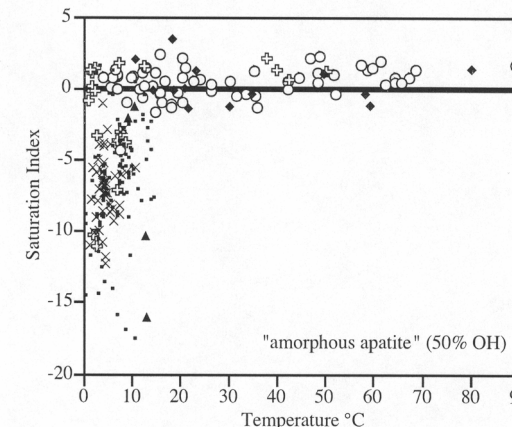


Fig. 8. Saturation index for "amorphous apatite" containing equal amounts of OH and F and as a function of temperature. Symbols refer to legend on Fig. 2.

their solubility. Values for iron hydroxide species activities carry much uncertainty, as indicated by large variations in published values for the iron hydroxide complex association. As a consequence SI values for any iron bearing mineral carry an error of an unknown magnitude. This error is probably not large for waters with a pH of less than 9 but it is apparently high for waters with a higher pH.

Alteration of basalt by <100°C ground waters largely involves plagioclase and olivine dissolution. The alteration products are principally quartz (chalcedony), various zeolites and clay minerals. Many trace metals are concentrated in the titanomagnetite of the basalt. The stability of this mineral in both surface- and ground waters reduces the mobility of these metals.

REFERENCES

- Arnórsson S. and Gíslason S. R. (1990) On the origin of low-temperature geothermal activity in Iceland. *Náttúrufræðingurinn* **60**, 39-56 (In Icelandic).
- Arnórsson S., Gíslason S. R., and Andrésdóttir A. (1995) Processes influencing the pH of geothermal waters. In *Proc. World Geothermal Congress*, Florence, Italy, 957-962.
- Arnórsson S., Gunnarsson I., Stefánsson A., Andrésdóttir A., and Sveinbjörnsdóttir Á.E. (2002) Major element chemistry of surface- and ground waters in basaltic terrain, N-Iceland. I. Primary mineral saturation. *Geochim. Cosmochim. Acta*, in press.
- Arnórsson S., Sigurdsson S., and Svavarsson H. (1982) The chemistry of geothermal waters in Iceland. I. calculation of aqueous speciation from 0° to 370 °C. *Geochim. Cosmochim. Acta* **46**, 1513-1532.
- Bjarnason J. O. (1994) The speciation program WATCH, version 2.1. Reykjavík, *National Energy Authority Report*, 7p.
- Clark J. S. (1955) Solubility criteria for the existence of hydroxyapatite. *Can J. Chem.* **33**, 1696-1700.
- Jóhannesson H. (1991) The mountains west of Eyjafjörður II. Reykjavík, *The Icelandic Tourist Association Yearbook 1991*, 246 p. (In Icelandic).
- Saemundsson K. and Fridleifsson I. B. (1980) Geothermal energy and geothermal investigations. *Náttúrufræðingurinn* **50**, 157-188. (In Icelandic with an English summary).

Askja - still going down

Erik Sturkell¹, Carolina Pagli^{2,3} & Freysteinn Sigmundsson²

¹Icelandic Meteorological Office, Reykjavík, ²Nordic Volcanological Institute, Reykjavík, ³Science Institute, University of Iceland.

The Askja volcano, located on the spreading plate boundary in north Iceland, consists of nested calderas, the latest formed in an eruption in 1875. The main Askja caldera is 8 km in diameter, and it was formed in the early Holocene. Several small eruptions have occurred since 1875, with the most recent in 1961. To follow the crustal deformation in Askja, GPS, InSAR and levelling techniques are used, those methods are independent from each other and all give a consistent picture of subsidence in the centre of the main caldera in recent years.

To monitor the crustal deformation in the Askja caldera a levelling line with twelve benchmarks was established in 1966 by Eysteinn Tryggvason. The profile was extended in 1968 to 30 benchmarks. The 30 points in the 1700m long profile are located radially from the centre of the main caldera. Between 1966 and 1972, the profile was levelled annually. During the period 1966 to 1972, alternating periods of uplift and subsidence were observed from levelling data, indicating deflation and inflation in the centre of the Askja main caldera (Tryggvason, 1989a and 1989b). No levelling was done in 1973 through 1982 and measurements were resumed in 1983 and have been conducted annually to 2002.

The first major GPS campaign with a dense network covering Askja was conducted in 1993 (Camitz *et al.*, 1995), when 24 stations were measured. In 1998 most of the 1993 GPS-network were re-measured. The observed surface deformation of Askja during 1983-1998 shows subsidence. The deformation signal obtained from the GPS and the levelling (tilt) measurements fits a "Mogi" model. Most of the deformation can be accounted for by a point source of pressure decrease (a Mogi model) near the centre of the main Askja caldera at a depth of 2.8 km.

An InSAR image spanning from 1992 to 1998 shows a concentric deformation pattern, associated with subsidence, north west of the lake Öskjuvatn, in the centre of the main caldera. The signal consists of 8 fringes, that correspond to 0.22 m change in the ground to satellite direction. The subsidence revealed by the interferogram fits reasonably with a "Mogi" point source. Preliminary forward modelling results in a best fitting location in the centre of the main caldera (65.04°N, 16.78°W) and at a depth d at 3.3 km. This is in good agreement with previous studies of by tilt (Rymer and Tryggvasson, 1993) and by GPS and tilt (Sturkell and Sigmundsson, 2000).

Subsidence in Askja can be modelled successfully with a Mogi type of point source with data from the three independently obtained data sets (tilt, GPS and InSAR). The models point to a shallow depth (2.5 - 3 km) in the centre of the caldera.

A time series since 1993 of the vertical displacement of two GPS-points relative the reference station DYNG shows continuous subsidence. The two stations are the two closest GPS -points to the subsidence center and consequently the most sensitive. The measurements indicate a slight decrease in the subsidence rate from 1993 to 2002. The reference station DYNG is located within the deformation field caused by the subsidence in the center of the main caldera, and its estimated subsidence is 0.016 m in the 1993 to 1998 period (Sturkell and Sigmundsson, 2000). The same pattern of a decrease in subsidence rate is seen in the levelling data. This rate of decrease is more obvious in the levelling data, as they span the time period 1983 to 2002.

Using the "Mogi" point source location presented by *Sturkell and Sigmundsson (2000)* and assuming it has been at the same place since the mid seventies, it is possible to calculate the total amount of subsidence by comparing the levelling result from 1972 and 2002. The "Mogi" point source model predicts the location (65.0448°N, 16.7805°W) and the depth d at 2,8 km, with those parameters fixed it is possible to find the vertical displacement h_0 over the point source.

The vertical displacement h_0 can be determined to be -1.86 m for the time period 1972 to 2002. Subsidence since 1972 has generated an integrated surface deflation volume of $2\pi h_0 d^2 \approx 0.092 \text{ km}^3$, using $h_0 = -1.86 \text{ m}$ and $d = 2.8 \text{ km}$. The corresponding volume change of the Mogi source is $2/3$, or about 0.061 km^3 .

The processes responsible for a subsurface volume reduction in volcanic areas include volume contraction and /or mass transport. Processes such as eruptions, lateral dyke injections, crystallisation and downwards draining will result in a volume reduction at shallow levels in the crust.

The eruption explanation can be ruled out in this case. Magma drainage into the Askja fissure swarm may accommodate some of subsidence. However, no rapid changes in the subsidence rate have been detected since 1983. The area with the most frequent earthquakes in the Askja region is not within the caldera but under Herðubreiðartögl and Herðubreið. The character of the earthquakes in that area is not in swarms, but rather single events and no seismic tremors or earthquake swarms suggestive of dyke injections has been recorded. No new ground fractures have been observed in the area. Cooling and contraction by degassing and crystallisation of the magma can be occurring. Such process is associated with 10-11% volume reduction. However, in post glacial time the Dyngjufjöll volcano complex has only produce lava's that are aphyric (G. E. Sigvaldason, personal communication, 2002) suggesting that no large volumes of magma rests and crystallise prior to an eruption. Some amounts of crystallisation is nevertheless likely occur, but just to a limited extent resulting in aphyric lavas (less than 5% of phenocrysts). Downward drainage into a deeper-seated magma reservoir might be possible. We suggest that magma solidification is an important process to explain some of the long-term subsidence in Askja but regional deformation and slow drainage of magma into the rift zone or downward to a deeper-seated magma reservoir most probably contributes to the volume reduction.

References

- Camitz, J., F. Sigmundsson, G. Foulger, C. -H. Jahn, C. Völksen, and P. Einarsson, Plate boundary deformation and continuing deflation of the Askja volcano, north Iceland, determined with GPS, 1987-1993, *Bull. Volcanol.*, 57, 136-145, 1995.
- Rymer, H., and E. Tryggvasson, Gravity and elevation changes at Askja, Iceland, *Bull. Volcanol.*, 55, 362-371, 1993.
- Sturkell, E., and F. Sigmundsson, Continuous Deflation of the Askja Caldera, Iceland, During the 1983-1998 Non-Eruptive Period. *J. Geophys. Res.*, 105, 25,671-25,684, 2000.
- Tryggvason, E., Ground deformation in Askja, Iceland: Its source and possible relation to flow of the mantle plume, *J. Volcanol. Geotherm. Res.*, 39, 61-71, 1989a.
- Tryggvason, E., Measurement of ground deformation in Askja 1966 to 1989, *Rep. 8904*, Nord. Volcanol. Inst., Univ. of Iceland, Reykjavík, 1989b.